Received: 31 May 2019 | Revised: 11 January 2020 | Accepted: 23 January 2020

DOI: 10.1002/nbm.4275

SPECIAL ISSUE RESEARCH ARTICLE

NMR IN BIOMEDICINE WILEY

Atlas-based GABA mapping with 3D MEGA-MRSI: Cross-correlation to single-voxel MRS

Ruoyun E. Ma[1,2,3] | James B. Murdoch[4] | Wolfgang Bogner[5] | Ovidiu Andronesi[6] | Ulrike Dydak[2,3]

[1]Center for Magnetic Resonance Research, Department of Radiology, University of Minnesota, Minneapolis, USA

[2]School of Health Sciences, Purdue University, West Lafayette, Indiana

[3]Department of Radiology and Imaging Sciences, Indiana University School of Medicine, Indianapolis, Indiana

[4]Canon Medical Research USA, Mayfield Village, Ohio

[5]High Field MR Center, Department of Biomedical Imaging and Image-guided Therapy, Medical University of Vienna, Vienna, Austria

[6]Athinoula A. Martinos Center for Biomedical Imaging, Department of Radiology, Massachusetts General Hospital, Harvard Medical School, Boston, Massachusetts

Correspondence
Ulrike Dydak, PhD, School of Health Sciences, Purdue University, 550 Stadium Mall Drive, West Lafayette, IN, 47906.
Email: udydak@purdue.edu

Funding information
NIEHS, Grant/Award Number: #R01 ES020529

The purpose of this work is to develop and validate a new atlas-based metabolite quantification pipeline for edited magnetic resonance spectroscopic imaging (MEGA-MRSI) that enables group comparisons of brain structure-specific GABA levels. By using brain structure masks segmented from high-resolution MPRAGE images and coregistering these to MEGA-LASER 3D MRSI data, an automated regional quantification of neurochemical levels is demonstrated for the example of the thalamus. Thalamic gamma-aminobutyric acid + coedited macromolecules (GABA+) levels from 21 healthy subjects scanned at 3 T were cross-validated both against a single-voxel MEGA-PRESS acquisition in the same subjects and same scan sessions, as well as alternative MRSI processing techniques (ROI approach, four-voxel approach) using Pearson correlation analysis. In addition, reproducibility was compared across the MRSI processing techniques in test–retest data from 14 subjects. The atlas-based approach showed a significant correlation with SV MEGA-PRESS (correlation coefficient r [GABA+] = 0.63, $P < 0.0001$). However, the actual values for GABA+, NAA, tCr, GABA+/tCr and tNAA/tCr obtained from the atlas-based approach showed an offset to SV MEGA-PRESS levels, likely due to the fact that on average the thalamus mask used for the atlas-based approach only occupied 30% of the SVS volume, ie, somewhat different anatomies were sampled. Furthermore, the new atlas-based approach showed highly reproducible GABA+/tCr values with a low median coefficient of variance of 6.3%. In conclusion, the atlas-based metabolite quantification approach enables a more brain structure-specific comparison of GABA+ and other neurochemical levels across populations, even when using an MRSI technique with only cm-level resolution. This approach was successfully cross-validated against the typically used SVS technique as well as other different MRSI analysis methods, indicating the robustness of this quantification approach.

KEYWORDS
GABA, MEGA-LASER, MEGA-PRESS, MRSI, validation

Abbreviations used: ATL, atlas; Cr, creatine; CSF, cerebrospinal fluid; CV, coefficient of variance; FA, flip angle; 4VX, four-voxel; FOV, field of view; FWHM, full width at half maximum; GABA, gamma-aminobutyric acid; Gln, glutamine; Glu, glutamate; Glx, glutamate + glutamine; GM, gray matter; GSH, glutathione; LASER, localization by adiabatic selective refocusing; MEGA, Mescher-Garwood (editing/edited); MM, macromolecule; MPRAGE, magnetization-prepared rapid gradient echo; MRSI, magnetic resonance spectroscopic imaging; NAA, N-acetylaspartate; NAAG, N-acetylaspartylglutamate; PCr, phosphocreatine; PRESS, point-resolved spectroscopy; ROI, region of interest; SD, standard deviation; SEM, standard error of the mean; SNR, signal-to-noise ratio; SV, single-voxel; SVS, single-voxel spectroscopy; TA, acquisition time; tCr, creatine + phosphocreatine; TE, echo time; TI, inversion time; tNAA, total NAA (N-acetylaspartate + N-acetylaspartylglutamate); TR, repetition time; VOI, volume of interest; WIP, work in progress; WM, white matter.

1 | INTRODUCTION

As the major inhibitory neurotransmitter in the human central nervous system, gamma-aminobutyric acid (GABA) plays a crucial role in the maintenance of regular brain function by balancing excitatory neuronal activity.[1,2] GABA is also deeply involved in controlling motor function, including motor decision speed,[3,4] motor learning and motor memory.[5,6] Moreover, abnormal GABA levels in various brain areas have been observed in a number of neurological, neuropsychiatric and neurodegenerative diseases.[7-9] Therefore, the study of GABA and the GABAergic system is of interest for both neurobiology in healthy brain and neuropathology in central nervous system disorders.

Proton magnetic resonance spectroscopy (MRS) provides the only noninvasive means to detect in vivo GABA levels, most commonly with the MEGA-PRESS sequence: Mescher-Garwood (MEGA) spectral editing[10] for GABA combined with single-voxel (SV) Point-RESolved Spectroscopy (PRESS) localization.[10-13] However, only one relatively large volume can be examined at a time, with a long acquisition time necessary to ensure data quality. By contrast, fast magnetic resonance spectroscopic imaging (MRSI) techniques can provide higher spatial resolution and a wider volume of interest (VOI) in an acceptable scan time. As such, moving on from SV MEGA-edited GABA measurements to MEGA-edited MRSI greatly benefits studies of diseases with possible alteration of GABA levels in multiple brain regions, as well as studies investigating GABA and the GABAergic system combined with other MRI techniques such as fMRI and diffusion tensor imaging.[14,15]

However, MEGA-edited fast GABA MRSI has been challenging. Compared with SV MRS, MRSI is affected more by B1 field inhomogeneity,[16] imperfect shimming across the scan volume, motion artifacts,[17] and frequency drift caused by scanner instability.[18,19] Moreover, the MRSI spectra along the edges of a PRESS-based VOI are affected more by chemical shift displacement error (CSDE). For MEGA-edited MRSI, these artifacts would compound any subtraction artifacts present in the difference spectra. Moreover, due to the low concentration of GABA, a high signal-to-noise ratio (SNR) is required, leading to a longer scan time and thus increased vulnerability to the above artifacts compared with nonedited MRSI scans. To reduce both scan time and the extent of these artifacts in MEGA-edited MRSI for GABA detection, a highly promising technique developed by Bogner et al,[20] known as MEGA-LASER 3D GABA MRSI, provides a robust approach for GABA mapping with a wider spatial coverage. This technique uses localization by adiabatic selective refocusing (LASER)[21] instead of PRESS localization to significantly reduce artifacts caused by B1 inhomogeneity, minimize CSDE and enhance SNR.[22] Real-time motion correction and shim updates with interleaved navigators improve the robustness, and spiral encoding effectively reduces the scan time.[23] This yields a more accurate measurement of the spatial variation of GABA in the central area of the brain and provides high reproducibility, as verified in a test–retest assessment.[24]

This improved GABA-edited 3D MRSI technique offers exciting possibilities for future studies of GABAergic systems: mapping of regional GABA variations, easier group comparisons across subject populations and better specificity to particular brain regions. For continuity with current studies, however, results should be compared with those from SV MEGA-PRESS, in particular, the correlation of neurochemical levels measured by the two techniques. Although the editing scheme is the same for the two sequences, the localization methods differ, as well as the bandwidths and shapes of both the excitation and refocusing pulses and the inclusion of shim and motion correction in the MEGA-LASER sequence. These different experimental parameters could possibly give rise to discrepancies between the spectra acquired by the two techniques. Furthermore, neither sequence as implemented here used macromolecule-symmetric editing[11,25] or neurochemical nulling[26,27] to account for coedited macromolecule (MM) signal at 3 ppm, the extent of which could also be a function of the sequence used. (In particular, differences in pulse timing for LASER vs. PRESS affect the extent of J-coupling evolution in both GABA and MM.) For these reasons, a careful assessment of the similarities and discrepancies between MEGA-LASER 3D MRSI and SV MEGA-PRESS spectroscopy is warranted.

The huge potential of this 3D GABA mapping technique also drives the need for a practical and reproducible approach to neurochemical quantification from brain regions and structures of interest. Until now, the main approaches used for MRSI data analysis of brain neurochemicals have fallen into three categories: (1) the use of manually chosen voxels from a portion of the region of interest (ROI) to represent the neurochemical levels of the entire region[24,28-30]; (2) atlas (ATL)-based techniques that use a transformation of the subject's MRSI data into Montreal Neurological Institute or other standard space (ATL) to assign exactly one structural label to each MRSI voxel[31-33]; and (3) voxel-based analysis by registering the neurochemical maps to a standard brain template to perform voxel-by-voxel statistical analysis[34] similar to the approaches used in functional MRI. The need for manual interaction in the first category could introduce user-dependent variation and requires time and training. For MRSI techniques that can achieve mm-level resolution, (2) and (3) are suitable approaches to provide statistical or group information on metabolite levels of particular brain structures. However, the transformation of lower resolution neurochemical maps into an ATL-space and classification of larger MRSI voxels to only one brain region is not accurate. However, the combination of high spatial resolution and robust GABA detection is difficult to achieve due to its low concentration.

We have therefore developed an ATL-based brain structure-specific[35] approach in the subject's native image space for automated regional quantification of neurochemical levels measured with MEGA-LASER 3D MRSI, which allows this GABA-mapping technique to be used in studies that aim at comparing GABA and other neurochemical levels in specific brain regions across populations or over time. The ATL method does not require a transformation into standard space and uses interpolated neurochemical maps for obtaining average brain structure-specific neurochemical concentration levels. The analysis method was used to facilitate the quantification of neurochemicals measured with MEGA-LASER 3D MRSI and to compare results with those from SV MEGA-PRESS for GABA, glutamate + glutamine (Glu + Gln ≡ Glx), N-acetyl aspartate + *N*-acetylaspartylglutamate (NAA + NAAG ≡ tNAA) and creatine + phosphocreatine (Cr + PCr ≡ tCr), which are the four main neurochemical signals

detected and quantified in a MEGA acquisition. In addition to the ATL-based quantification approach, a matched ROI-based method for quantifying neurochemical signals measured with MRSI was used to directly compare values obtained from the same location with those measured by single-voxel spectroscopy (SVS). These two automated methods and the SVS measurement were further compared with the traditionally used manual approach of averaging over selected MRSI voxels. Finally, the intrasubject reproducibility of the new ATL approach was evaluated on test–retest GABA MRSI data from an earlier study.[24]

2 | METHODS

2.1 | Subjects

Twenty-one healthy male subjects (age: mean [SD] = 41 [11] years; range: 22–54 years) were recruited for the study. The study was approved by the Institutional Review Board of Indiana University. Written and informed consent forms were signed by all subjects, none of whom presented with any neurological, neurodegenerative or psychiatric disorders.

2.2 | MRI and ROI/VOI placement

The MRI/MRS examinations were performed on a clinical 3 T MR scanner (Tim Trio, Siemens Healthcare, Erlangen, Germany) equipped with a 32-channel receive head coil. MPRAGE images (TR/TE/TI = 2300/4.21/900 ms, FA = 9°, FOV = 160 x 240 x 256 mm, 1 x 1 x 1 mm resolution, TA = 6.38 minutes) were acquired for further image processing to obtain segmented brain structures.

The SVS ROIs were centered on the right thalamic region with a size of 30 x 25 x 25 mm^3 (18.7 ml) (Figure 1A) following the prescription of our former GABA MRS studies on movement disorders.[36-38] The thalamus was selected for SVS measurement for two reasons. First, the thalamus

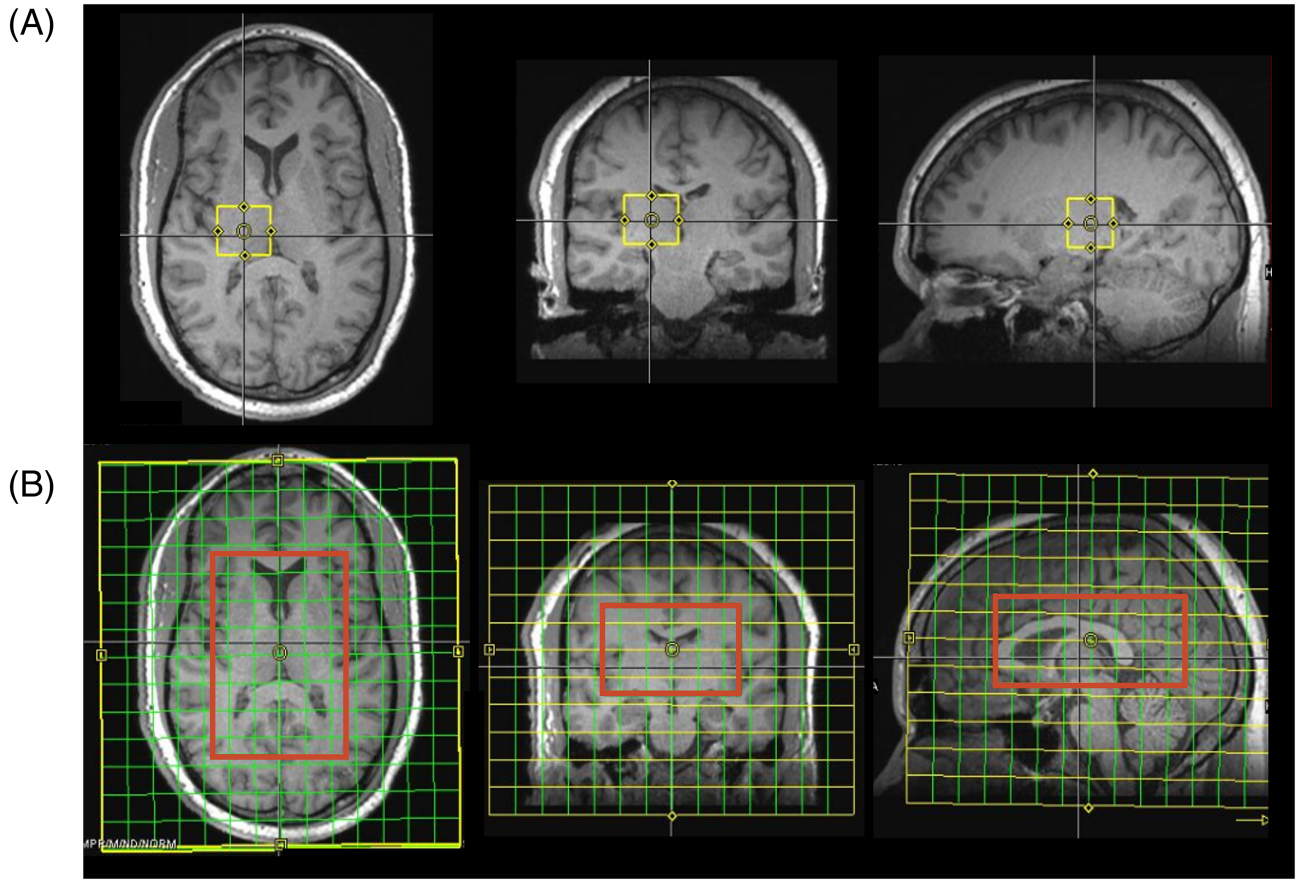

FIGURE 1 (A) Localization of a 30 x 25 x 25 mm SV ROI depicted on axial, coronal and sagittal 3D T1-weighted images in the thalamic region. (B) FOV (200 x 200 x 170 mm) and VOI placement for 3D MRSI. The yellow box represents the FOV; the red box displays the VOI; green grids indicate the spatial acquisition matrix

is rich in GABAergic neurons with its own GABAergic local circuits[39]; it also receives GABA input from the substantia nigra[40] and internal pallidum.[41] Second, the thalamus is a relatively large brain structure with a shape that fits easily (but not perfectly) in an SVS voxel.

The 3D MRSI VOIs were centered on the basal ganglia region and included the thalamus (Figure 1B). The FOV used for all subjects was 200 x 200 x 170 mm, which covered the whole brain and skull. The VOIs were chosen according to the size and shape of the brain of each subject, ranging from 70 to 75 mm in the left–right direction, 80 to 120 mm in the anterior–posterior direction and 45 to 55 mm in the superior–inferior direction. The scan matrix size was 14 x 14 x 12 interpolated to 16 x 16 x 16. The nominal acquisition resolution was 2.89 ml.

2.3 | MRS and MRSI acquisition

The protocols for the SV MEGA-PRESS and MEGA-LASER 3D MRSI scans were determined based on commonly used parameter sets for each acquisition.[20,24,42,43] This was because our goal was to compare results from the two sequences when they were both adjusted for optimized performance.

The MEGA-PRESS Siemens WIP sequence was used for the SV MEGA-PRESS scans, with the editing frequency centered on 1.90 ppm for edit-ON spectra and 7.50 ppm for edit-OFF spectra. The other sequence settings were TR/TE = 2000/68 ms, 128 averages for edit-ON and 128 averages for edit-OFF, a Gaussian editing pulse with a specified bandwidth of 44 Hz (but reportedly closer to 60 Hz in actuality),[44] vector size 2048, acquisition bandwidth 2000 Hz, delta frequency set at −1.7 ppm relative to water (ie, localization pulses applied at ~3.0 ppm to optimally target tCr) and an acquisition time of 8.40 minutes. A reference scan without water suppression was acquired for every SVS scan for eddy current correction. Advanced automatic B0 shimming combined with occasional manual tweaking to achieve optimal results was used to shim the voxels. The full width at half maximum (FWHM) value of the water peak was measured and recorded as the linewidth value for each spectroscopy scan.

For MEGA-LASER 3D MRSI, the two editing frequencies (1.9/7.5 ppm) were the same as those used in SV MEGA-PRESS. Other acquisition parameters included TR/TE = 1600/68 ms, four dummy scans, 16 weighted averages for edit-ON and 16 for edit-OFF, a Gaussian editing pulse with a specified bandwidth of 60 Hz, vector size 512, acquisition bandwidth 1250 Hz, delta frequency – 1.7 ppm and an acquisition time of 19.44 minutes. Separate water-unsuppressed reference scans were not acquired because of time limitations. The B0 shimming procedures were performed in the same way as SV MEGA-PRESS. It is worth noting that the MRSI VOIs were chosen to ensure good shimming results; consequently, the SVS ROI could not always be entirely included within the MRSI VOI.

Because the edited peaks at 3.0 ppm from the two sequences in this study contain GABA, coedited MMs and homocarnosine (a dipeptide consisting of GABA and histidine),[45] the measured GABA signal is denoted as GABA+.

2.4 | Spectral quantification

For both SVS and MRSI, the ON, OFF and subtracted difference spectra were reconstructed online and were exported offline for spectral fitting and quantification. The details of MRSI reconstruction can be found in Bogner et al.[20] All spectra were quantified with LCModel V6.3-1B.[46] For SV MEGA-PRESS, the basis sets for LCModel spectra fitting were generated from density matrix simulations of the sequence using software developed by Murdoch[47] with published and corrected values for chemical shifts and J-coupling constants.[48,49] Spin evolution during the MEGA editing pulses was taken into account, but the localization pulses were assumed to be hard pulses. Twenty neurochemicals were included in the edit-OFF basis set: GABA, Glu, Gln, NAA, NAAG, Cr, PCr, glutathione (GSH), glycerophosphorylcholine, phosphorylcholine, myo-inositol, scyllo-inositol, lactate, alanine, aspartate, taurine, glucose, phosphorylethanolamine, ascorbate and glycine. Of these, only six were included in the difference spectrum basis set: GABA, Glu, Gln, NAA, NAAG and GSH. To be compatible with the MRSI results, no water scaling or cerebrospinal fluid (CSF) correction was applied. Small relaxation corrections to neurochemical ratio values were also omitted. For MEGA-LASER 3D MRSI, the basis sets were simulated based on the radiofrequency pulses and MEGA-LASER scheme using GAMMA, as previously described.[20,24] The analysis range for spectral fitting was 1.4–4.2 ppm for MRSI and 0.2–4.0 ppm for SVS. Neurochemical levels of GABA+ and Glx (measured from difference spectra for better fitting quality and smaller Cramer-Rao Lower Bounds [CRLB] values than obtained from edit-OFF spectra), tNAA and tCr (measured from edit-OFF spectra), plus the ratios GABA+/tCr, tNAA/tCr and Glx/tCr, were included in the comparison.

2.5 | ATL-based approach

Neurochemical maps within the VOI were generated from LCModel fitting results using a Matlab (MathWorks, Natick, MA) 2014 script,[20] interpolated into higher resolution (1 x 1 x 1 mm^3) and registered to MPRAGE images using Medical Imaging NetCDF. For GABA+, only voxels with CRLB values smaller than 30% were included in the analysis; for tNAA, tCr and Glx, only voxels with CRLB smaller than 20% were included. When calculating ratios, the voxels included in the analysis were the ones that satisfied the quality control criteria of both neurochemicals. The MPRAGE

images were processed with FreeSurfer to perform brain structure segmentation.[50,51] The thalamus was extracted and used as a mask to be registered to the neurochemical maps. An example of the thalamus mask registered on T1-weighted images as well as the MRSI VOI from the same subject is shown in Figure 2A. Averaged values from the region within the thalamus mask on the neurochemical maps were calculated to represent the mean level of each neurochemical within the thalamus. This is denoted as the ATL-based approach.

2.6 | ROI-based approach

In addition to the ATL-based approach, the SV MEGA-PRESS ROIs were registered to MRSI-based neurochemical maps. Averaged values were calculated from the region within the ROI on the maps to compare with levels quantified from SV MEGA-PRESS spectra. This approach is denoted as the ROI-based approach and was applied to this study to enable a more direct comparison of the neurochemical levels measured by the two localization techniques, because the SVS ROI included more than just the thalamus.

2.7 | Four-voxel approach

In this study, we also applied the widely used method of manually choosing voxels for metabolite quantification. First, the raw neurochemical maps generated after LCModel quantification were registered to T1-weighted images without any interpolation. Second, four neighboring voxels

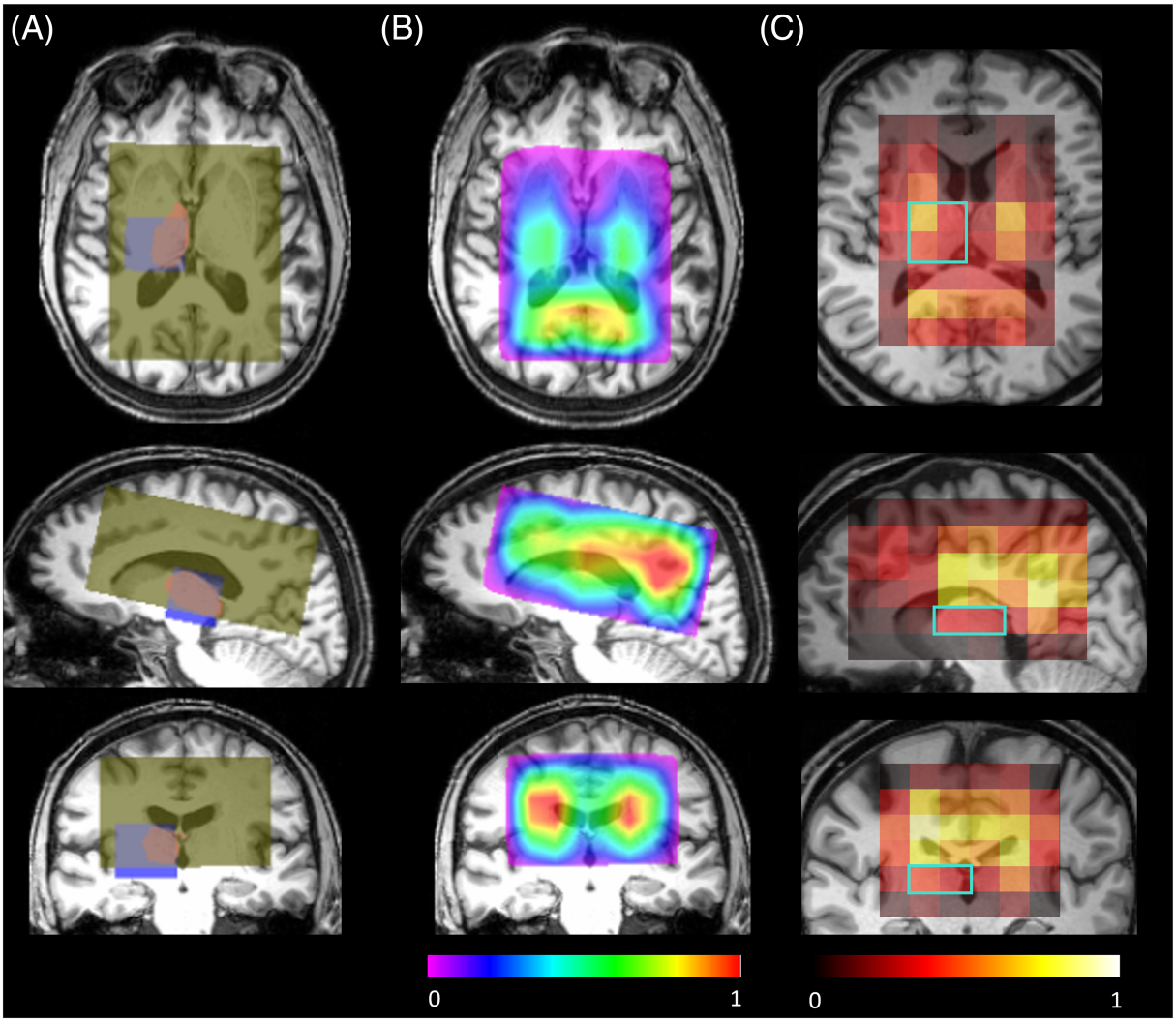

FIGURE 2 (A) Example of MRSI VOI (brown), thalamus mask (red) and SV ROI mask (blue) overlaid on anatomical images; (B) representative GABA+ map overlaid on anatomical images in axial, sagittal and coronal planes; (C) an example of four manually picked voxels shown in the turquoise box (4VX approach) overlaid on the GABA+ map and anatomical images to quantify thalamic neurochemical levels

from the thalamic region and within the SVS ROI (but not on the edge of the MRSI VOI) were selected for each subject. Finally, the neurochemical levels from these voxels were averaged for further statistical analysis. Figure 2C shows an example of this approach applied on one dataset. This is denoted as the four-voxel (4VX) approach.

2.8 | Test–retest reproducibility of the ATL-based approach

To evaluate the intrasubject reproducibility of the ATL-based approach, a test–retest analysis was performed retrospectively using a dataset containing 14 healthy volunteers from an earlier study[24] that used the same MRSI acquisition technique and parameters. Applying the ATL-based approach on this data, the values of GABA+/tCr, tNAA/tCr and Glx/tCr from the right thalamus were calculated. For all ratio values, mean and standard error across all subjects from each scan session, ie, test or retest, as well as the intersession coefficient of variance (CV) from every subject were calculated. Bland–Altman plots were generated to visualize the agreement between the test and retest sessions (see the supporting information). Additionally, we assessed CVs for the size of the volume that passed the CRLB-based quality control criteria in each dataset to ensure that the calculated metabolite ratios were from the same volume of the thalamus.

2.9 | Comparison between MEGA-LASER 3D MRSI and SV MEGA-PRESS

The ATL-based approach was validated by comparing mean neurochemical levels from the thalamus acquired using MRSI with those acquired with SVS. The neurochemical levels from ROI-based and 4VX approaches were also compared with SVS.

The ATL-based analysis was performed using an in-house package written in Matlab 2014a, which in turn was interfaced with LCModel. The overlaps between (1) the SVS ROI and the MRSI VOI, (2) the SVS ROI and the thalamus, and (3) the thalamus and MRSI VOI were calculated to determine if the main source of the signals compared came from the same brain region. The overall analysis pipeline is illustrated in Figure 3.

For statistical comparisons, normality of each variable was tested using the Shapiro–Wilk test, as recommended by Razali and Wah.[52] Mean values and standard errors of GABA+/tCr, tNAA/tCr and Glx/tCr were calculated. Paired t-tests were applied to compare the GABA+/tCr, tNAA/tCr and Glx/tCr values measured by SV MEGA-PRESS versus those from MEGA-LASER 3D MRSI quantified with the aforementioned three approaches, as well as to compare the ATL-based approach and the other two quantification methods used for MRSI. Bland–Altman plots were generated to visualize any systematic bias between SVS and MRSI measurements. The cross-validation between the neurochemical levels measured by SVS and MRSI was conducted using two steps. First, correlations of the neurochemical levels as well as their ratio to tCr measured by MEGA-LASER 3D MRSI and SV MEGA-PRESS were examined using Pearson correlation analysis (for each analysis approach separately). Second, for GABA+/tCr, tNAA/tCr and Glx/tCr, linear regression was performed with the intercept set to zero. The hypothesis is that the neurochemical levels normalized to tCr as measured by different techniques should approach an identity line in such a regression. For all statistical tests, results with *P*-values less than 0.05 were considered to be significant. The statistical analysis was performed using SAS9.3 (2011) (SAS Institute, Cary, NC).

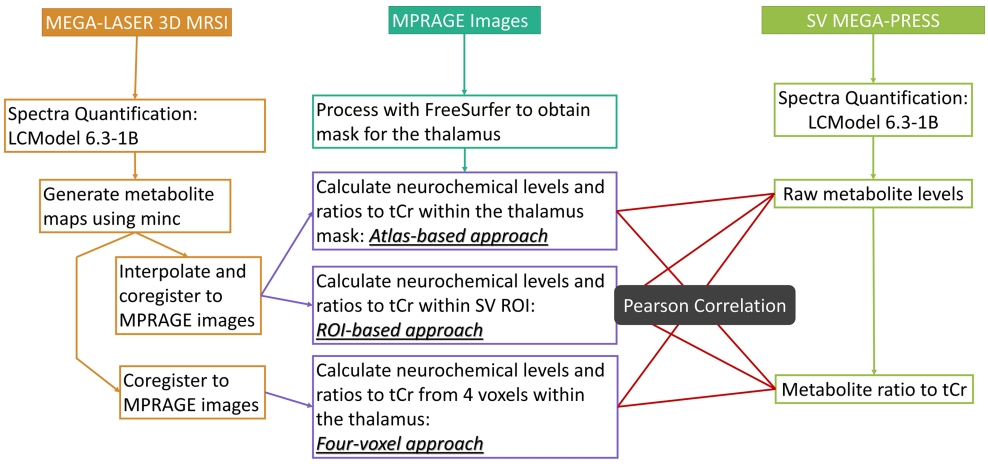

FIGURE 3 Postprocessing pipeline for calculating neurochemical levels and their corresponding ratios to tCr, and comparison of the measurements from SV MEGA-PRESS and MEGA-LASER 3D MRSI

3 | RESULTS

3.1 | Spatial overlaps between the SVS ROI, MRSI VOI and thalamus

The VOI of 3D MEGA-LASER MRSI covered 100% of the thalamus mask, but only 93.8% (6.6%) (mean [SD]) of the SV MEGA-PRESS ROI, mainly due to a slightly more superior placement of the MRSI VOI. The large overlap between the SV ROI and the MRSI VOI, indicating the same source for most of the observed signal, provides a basis for comparing the results acquired with the two techniques. The thalamic mask occupied on average only 30% (5%) of the SVS ROI due to the ROI's cuboid shape. (The rest of the SV volume is composed of white matter [WM] [40%], ventricle dorsal column [10%] and putamen [4.5%], as well as parts of other nearby structures including pallidum, lateral ventricle, hippocampus, amygdala, choroid plexus, CSF and a very small area of the cortex.) Vice versa, the SVS ROI also did not cover the full thalamic mask, but only 81.2% (7%) of it. This was caused by the fact that the most anterior and posterior parts of the thalamus were not included in the SV ROI, as shown in Figure 2A.

3.2 | Data quality

Representative spectra from SV MEGA-PRESS acquisitions and 3D MEGA-LASER MRSI acquisitions appear in Figure 4A,B. All difference spectra showed good data quality with clearly resolved GABA+ peaks at 3 ppm, except for one subject with excessive motion that yielded a poor MEGA-PRESS spectrum and two subjects with poor MEGA-PRESS water suppression. These datasets were therefore excluded from the ones used for comparison. The mean values (SD) of the FWHM values of the water peaks measured on site were 19.7 (3.1 Hz) for the SV ROI and 23.4 (2.9 Hz) for the MRSI VOI, indicating reliable data quality. To visually compare MRSI data from the thalamic region with SV results, MRSI spectra from voxels which were fully included in the region covered by the SV ROI were averaged and plotted relative to the corresponding SV spectra; examples from seven different subjects are displayed in Figure 4C. In line with the comparisons between PRESS and LASER localization from Bogner et al,[20] spectra acquired with MEGA-LASER MRSI showed better SNR than MEGA-PRESS SV spectra using commonly applied acquisition protocols. Representative maps for GABA+ in axial, sagittal and coronal views are displayed in Figure 2B.

3.3 | Test–retest reproducibility of the ATL-based approach

The mean and standard error of mean (SEM) values of GABA+/tCr, tNAA/tCr and Glx/tCr from test and retest sessions using the ATL-based approach, as well as the size of the volume (in mm^3) included in the calculation, are listed in Table 1A. The CV values used to characterize

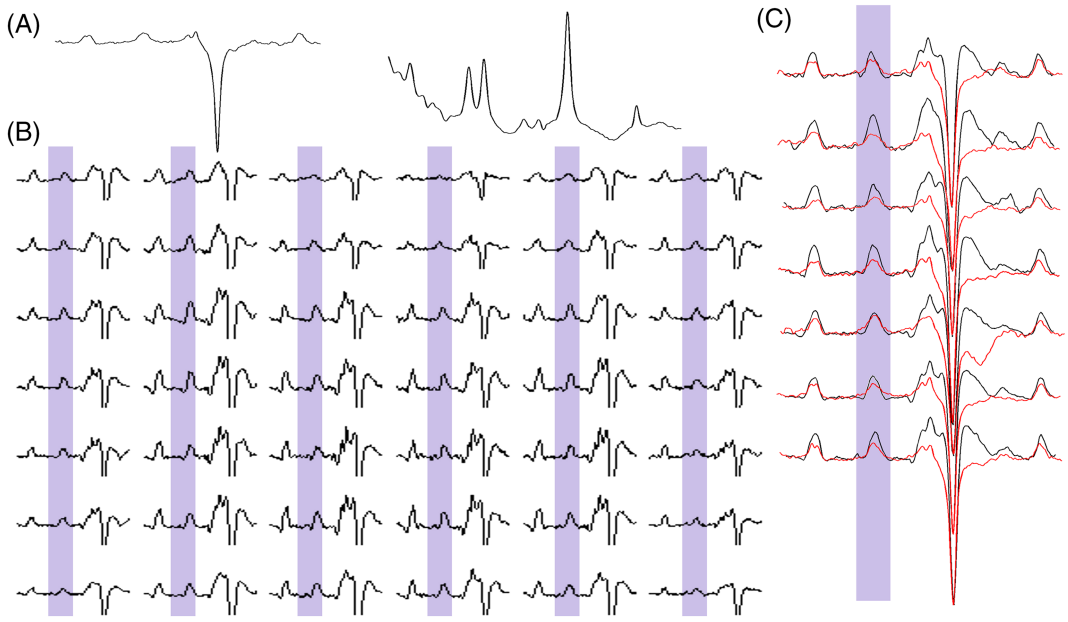

FIGURE 4 (A) Representative difference spectrum (left) and edit-OFF spectrum (right) acquired with SV MEGA-PRESS; (B) representative difference spectra from the VOI within one axial slice; (C) examples from seven subjects showing the overlay of the averaged spectra from the MEGA-LASER 3D MRSI voxels within the thalamus (black) and spectra acquired from SV MEGA-PRESS (red), with negative NAA and baseline aligned

TABLE 1A Mean and standard error of mean (SEM) across all subjects for the neurochemical levels and the size of the thalamus included in the calculation of GABA+/tCr, tNAA/tCr and Glx/tCr from each test–retest session using the atlas-based approach. The somewhat smaller average volumes for GABA+/Cr compared with the other ratios are an indication that some voxels did not meet the Cramer-Rao lower bounds (CRLB)-based quality control criteria

	Neurochemical levels		Size of volume (mm^3)	
	Test	Retest	Test	Retest
GABA/tCr	0.27 (0.006)	0.26 (0.007)	7573 (171)	7584 (182)
tNAA/tCr	1.73 (0.030)	1.71 (0.029)	7667 (187)	7776 (206)
Glx/tCr	1.53 (0.026)	1.53 (0.023)	7653 (214	7745 (199)

TABLE 1B Coefficient of variance (CV) values for intrasubject variability of neurochemical levels and the size of the thalamus included in the calculation of GABA+/tCr, tNAA/tCr and Glx/tCr using the atlas-based approach. Median and 25% to 75% of CV values are shown

	CV of neurochemical levels		CV of size of volume (mm^3)	
	Median	25–75 percentile	Median	25–75 percentile
GABA/tCr	6.30	1.54–9.58	2.08	0.84–4.26
tNAA/tCr	0.60	0.24–1.29	2.21	0.91–4.08
Glx/tCr	2.35	1.60–3.88	1.62	1.06–4.08

intrasubject variability for GABA+/tCr, tNAA/tCr and Glx/tCr, as well as the CV values for the size of the volume included in the calculation, are specified in terms of median and 25%–75% percentiles in Table 1B. Closely matching mean ratio values and low CV values between the two sessions indicate high intrasubject reproducibility of neurochemical levels and thalamic volume sizes included in the calculation.

3.4 | Cross-validation between MRSI and SVS

Descriptive statistics for GABA+/tCr, tNAA/tCr and Glx/tCr are shown in Table 2A, with *P*-values from paired t-tests. The mean CRLB from LCModel fitting is presented in Table 2B for each neurochemical and each analysis technique. Bland–Altman plots for these ratio values are displayed in Figure 5 to visualize the bias between SVS and MRSI quantified with three different approaches. For GABA+/tCr and tNAA/tCr, the mean difference is close to zero. By contrast, a significantly nonzero mean difference is seen for Glx/tCr. Correlation analysis results between the two localization techniques, as well as between the three different quantification approaches for MRSI, are listed in Table 3. The GABA+ values acquired with MRSI and quantified with the ATL-based approach are significantly and linearly correlated with GABA+ values quantified by the

TABLE 2A descriptive statistics (mean and standard error of mean [SEM]) for GABA/tCr, tNAA/tCr and Glx/tCr measured by the two acquisition techniques. *P*-values from paired t-tests compare the metabolite ratios obtained by MRSI quantified with the atlas (ATL)-based brain-structure specific approach versus single-voxel spectroscopy (SVS), as well as with the two other MRSI quantification methods: Matched ROI-based and four-voxel (4VX)

	GABA+/tCr	tNAA/tCr	Glx/tCr
Descriptive statistics (mean ± SEM)			
SVS	0.29 ± 0.015	1.61 ± 0.039	1.07 ± 0.038
MRSI (ATL)	0.23 ± 0.007	1.63 ± 0.024	1.52 ± 0.024
MRSI (ROI)	0.25 ± 0.007	1.70 ± 0.025	1.49 ± 0.022
MRSI (4VX)	0.26 ± 0.011	1.72 ± 0.027	1.50 ± 0.023
P-values from paired t-test			
ATL vs. SVS	0.004	0.54	7.10E-10
ATL vs. ROI	0.25	0.07	0.45
ATL vs. 4VX	0.04	0.01	0.67
4VX vs. SVS	0.22	0.01	1.38E-09
ROI vs. SVS	0.02	0.05	2.08E-09

TABLE 2B Cramer-Rao lower bounds (CRLB) (mean ± SEM) of GABA+, tNAA, tCr and Glx measured with SVS and MRSI

	GABA+	tNAA	tCr	Glx
SVS	13 ± 0.7	2 ± 0.8	3 ± 0.2	8 ± 0.5
MRSI (ATL)	20 ± 0.6	3 ± 0.1	3 ± 0.1	12 ± 0.5
MRSI (ROI)	19 ± 0.4	4 ± 0.1	3 ± 0.1	13 ± 0.4
MRSI (4VX)	16 ± 0.8	2 ± 0.1	3 ± 0.1	9 ± 0.4

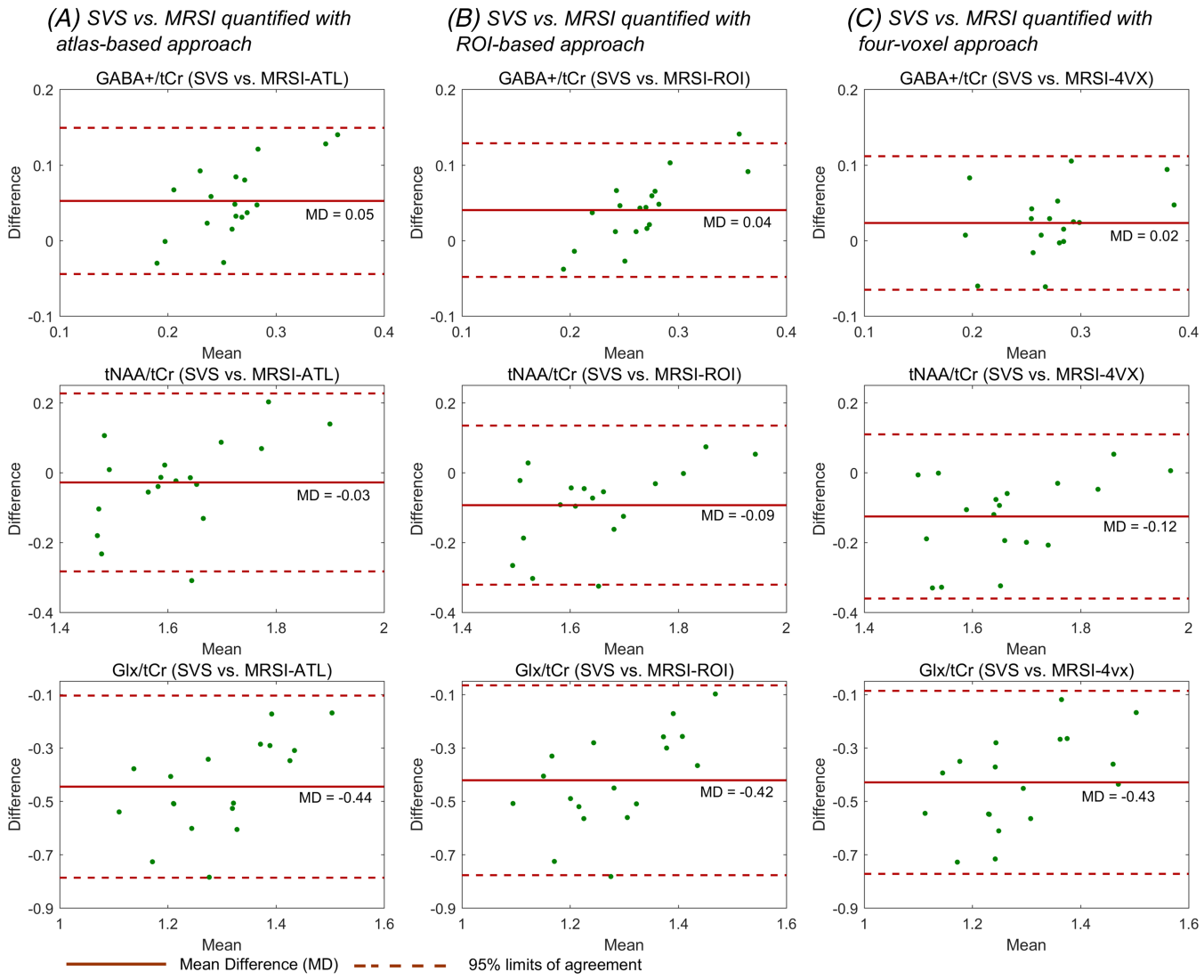

FIGURE 5 Bland–Altman plots for GABA+/tCr, tNAA/tCr and Glx/tCr from the SVS measurement and the three MRSI quantification approaches ((A) ATL, (B) ROI and (C) 4VX), showing the mean difference (MD, red solid lines) and 95% confidence intervals of limits of agreement (red dotted lines)

other two MRSI analysis approaches, as well as the values obtained with SVS, as indicated by the correlation coefficients r and associated probability values (SVS: r [*P*] = 0.63 [0.005]; ROI-based approach: r [*P*] = 0.93 [<0.0001]; 4VX approach: r [*P*] = 0.91 [<0.0001]). Similarly, significant correlations were also seen for GABA+/tCr, tNAA, tNAA/tCr and tCr. No such relationship was found for Glx or Glx/tCr. For GABA+ and GABA+/tCr, the linear correlations between the values obtained with the ROI-based approach and the values from SVS are slightly more significant than the analogous relationships for the ATL-based and 4VX approaches, as indicated by larger r-values (and smaller *P*-values) for the latter pairs in Table 3. Results for the three different MRSI analysis schemes are strongly correlated with each other for all neurochemicals and neurochemical ratios of interest.

TABLE 3 Correlation coefficients (and *P*-values) for metabolite levels and ratios measured with single-voxel spectroscopy (SVS) versus values obtained with the three MRSI analysis methods: Atlas (ATL)-based, ROI-based and four-voxel (4VX), as well as correlations between the three MRSI quantification approaches

	SVS vs. MRSI (ATL)	SVS vs. MRSI (ROI)	SVS vs. MRSI (4VX)	MRSI (ATL) vs. MRSI (ROI)	MRSI (ATL) vs. MRSI (4VX)	MRSI (ROI) vs. MRSI (4VX)
GABA+	0.68 (0.002)	0.78 (<0.0001)	0.73 (0.0005)	0.93 (<0.0001)	0.93 (<0.0001)	0.95 (<0.0001)
tNAA	0.77 (0.0002)	0.80 (0.0002)	0.65 (0.003)	0.92 (<0.0001)	0.87 (<0.0001)	0.91 (<0.0001)
tCr	0.48 (0.04)	0.41 (0.08)	0.54 (0.02)	0.93 (<0.0001)	0.91 (<0.0001)	0.92 (<0.0001)
Glx	0.21 (0.39)	0.12 (0.63)	0.20 (0.43)	0.93 (<0.0001)	0.89 (<0.0001)	0.94 (<0.0001)
GABA+/tCr	0.63 (0.005)	0.76 (0.0003)	0.70 (0.001)	0.93 (<0.0001)	0.91 (<0.0001)	0.93 (<0.0001)
tNAA/tCr	0.61 (0.007)	0.71 (0.001)	0.68 (0.002)	0.94 (<0.0001)	0.92 (<0.0001)	0.96 (<0.0001)
Glx/tCr	0.28 (0.25)	0.21 (0.40)	0.29 (0.23)	0.93 (<0.0001)	0.83 (<0.0001)	0.86 (<0.0001)

Scatter plots for the regression analysis of GABA+/tCr, tNAA/tCr and Glx/tCr between SVS and MRSI measurements are displayed in Figure 6, with regression lines, regression equations, 95% confidence intervals, 95% confidence limits and identity lines (SVS values = MRSI values). The fitted regression equation and R-squared are also displayed. For GABA+/tCr, data points from the ATL-based and ROI-based approaches are noticeably offset from the identity line compared with data points from the 4VX approach. The data points from Glx/tCr are far from the identity line.

4 | DISCUSSION

This study demonstrates the performance of an automated ATL-based approach for quantifying the average metabolite concentrations of specific brain structures from lower resolution MRSI, as in GABA-edited MRSI, that has been developed for use in studies that aim to compare brain structure-specific neurochemical concentrations across populations. The new approach has been compared with other MRSI analysis approaches, and was cross-validated with SV MEGA-PRESS data for one brain structure; in this case, the thalamus. The same approach can similarly be used to investigate the neurochemical concentration in other brain structures enclosed by an MRSI VOI. Specifically, results from 3D MEGA-LASER MRSI and SV MEGA-PRESS have been compared and cross-validated by examining the correlations between GABA+, tNAA, tCr and Glx levels plus corresponding ratios to tCr as measured with the two scan techniques in the same brain region. These are the most commonly reported quantities from MEGA-edited MRS techniques, and our findings provide a reference for evaluating the influence of different sequences when comparing results from different studies. Good spectral quality was achieved for both techniques. The results demonstrate a linear relationship between neurochemical levels from SV MEGA-PRESS and 3D MEGA-LASER MRSI acquisitions, with the exception of Glx, which has different coupling behavior and chemical shifts than GABA.

4.1 | Comparison of measured neurochemical ratio levels with other studies

The average thalamic neurochemical levels normalized to tCr measured from the ATL approach in this study (GABA+/tCr = 0.23; tNAA/tCr = 1.62; Glx/tCr = 1.53) are similar to the values measured by Hnilicová et al[24] (GABA+/tCr = ~ 0.28; Glx/tCr = ~ 1.6) using the same MRSI sequence. A much wider range of neurochemical levels has been reported using SVS MEGA-PRESS, with GABA+/tCr values ranging from 0.14[37] and 0.17[53] to 0.3[54] and 0.39[55] in healthy controls. Thus, our measurements agree with the thalamic metabolite levels measured by MRS/MRSI from other studies.

Individual measurements from our study yielded a range of neurochemical levels, especially for thalamic GABA+/tCr (0.17–0.29 for MRSI with the ATL approach, 0.18–0.43 for SVS). One source for the intersubject variability in thalamic GABA+/tCr values could originate from the thalamus itself, which is close to the ventricles and other sources of susceptibility differences, thereby resulting in higher variability. This effect was also observed by Hnilicová et al,[24] with a broader 95% confidence interval seen for the mean values in thalamus voxels compared with those for cortical voxels. In addition, the healthy subjects in our study were recruited from a wide range of occupations, including some workers from a local factory who were exposed to heavy metals in welding fumes, which has been shown to be associated with higher thalamic GABA/tCr levels.[37,38] We did not try to exclude these subjects because our hypothesis is that the two techniques (SVS and MRSI) should provide similar and well-correlated results over a wide range of neurochemical levels.

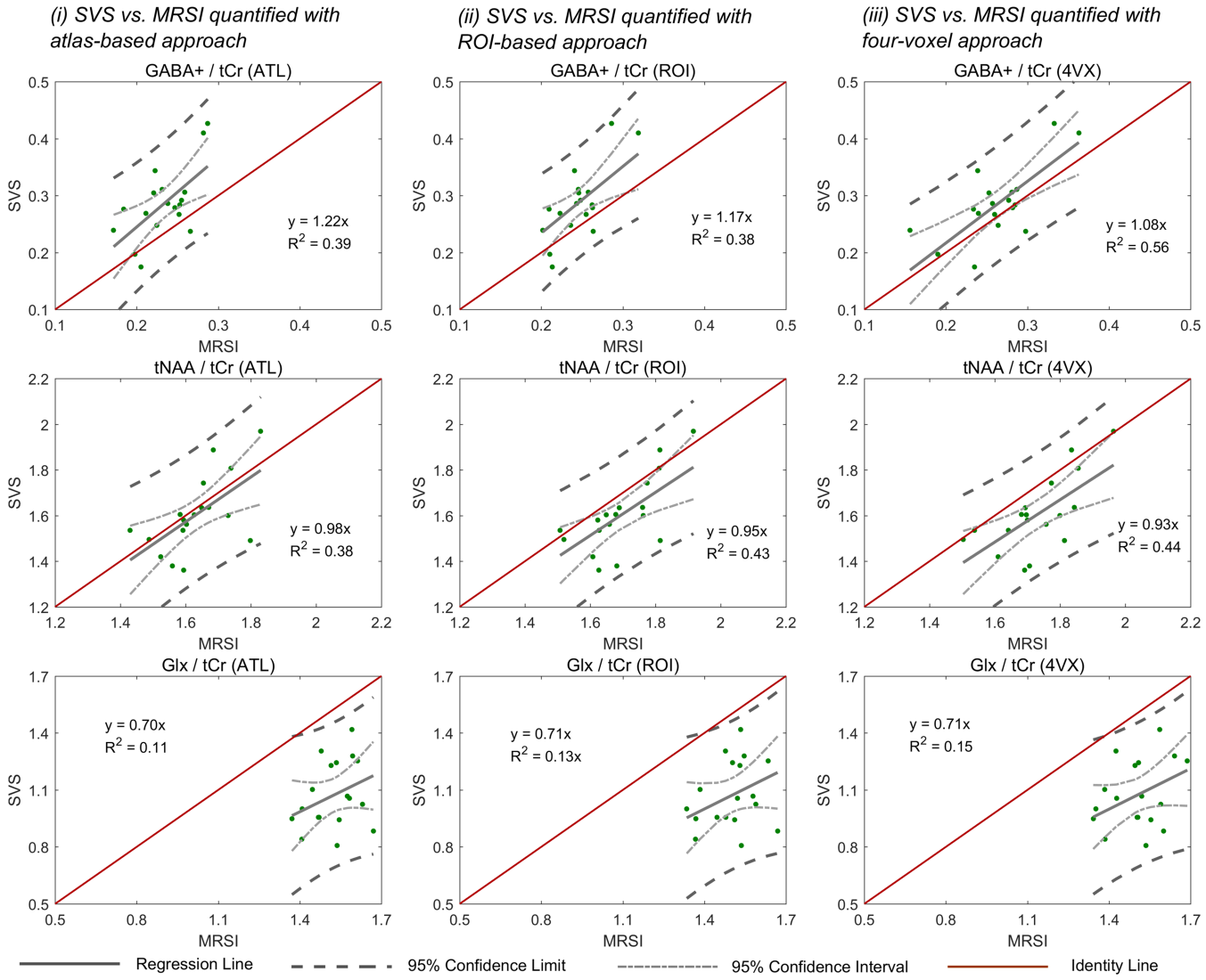

FIGURE 6 Scatter plots with lines of regression through the origin, 95% confidence intervals and 95% confidence limits for (i) neurochemical ratios measured with SVS versus neurochemical ratios measured with MRSI quantified with the atlas (ATL)-based approach; (ii) neurochemical ratios measured with SVS versus neurochemical ratios measured with MRSI and quantified with the ROI-based (ROI) approach; (iii) neurochemical ratios measured with SVS versus neurochemical ratios measured with MRSI quantified with the four-voxel (4VX) approach. The regression equations and the R-squared (R2) of the regression for GABA+/tCr, tNAA/tCr and Glx/tCr are displayed in the plots accordingly

4.2 | Reproducibility of the ATL-based approach

The test–retest analysis, performed on the data from Hnilicová et al,[24] showed the high reproducibility of the ATL-based approach. Compared with the reproducibility values reported by Hnilicová et al,[24] who used manually chosen MRSI voxels for structural neurochemical quantification, our ATL-based approach yielded lower CV values on the same test–retest MRSI data. For the ATL-based approach, the median GABA+/tCr CV was 6.30, with a 25%–75% percentile range of 1.54 to 9.58 compared with 8.1 (percentile range = 3.6–14.1) reported by Hnilicová et al[24]; for Glx/tCr, the median was 2.35 with a 25%–75% percentile range of 1.60–3.88 compared with 5.6 (percentile range = 2.5–10.0). An important reason for this improvement in reproducibility could be a better definition of the thalamic volume. With a larger coverage of the thalamus for the ATL-based approach (7664 vs. 1660 mm^3 for the manual approach used by Hnilicová et al),[24] the calculated neurochemical levels better represent the average values of the entire thalamus, with less variability resulting from substructures in the thalamus that could affect the calculated neurochemical levels when manually picking a much smaller part of the thalamus.

4.3 | Comparison of MEGA-LASER 3D MRSI with SV MEGA-PRESS

In this study, a practical ATL-based approach using FreeSurfer was developed and applied to compare the neurochemical levels measured by MEGA-LASER 3D MRSI and SV MEGA-PRESS. The approach was validated based on the significant correlations found for GABA+, tNAA, tCr, GABA+/tCr and tNAA/tCr levels.

Although GABA+/tCr and tNAA/tCr both showed significant correlation between the measurements from the two localization techniques, the plots in Figures 5 and 6 illustrate that GABA+/tCr measured by MRSI is generally lower than GABA+/tCr measured by SVS, especially for ATL- and ROI-based approaches. One reason for this distribution could be that, on average, the thalamus only occupied 30% of the SV ROIs, with the other space mostly filled with WM (40% of the ROI size), as well as CSF and a small portion of the putamen. In addition, as noted earlier, the most anterior and posterior portions of the thalamus stick out beyond the SV ROI. Despite its relatively compact shape, the thalamus is not a rectangular cuboid. As such, MRSI with the ATL-based quantification approach should be able to provide more accurate thalamic GABA+ measurements. Another contributing factor may be the difference in how much coedited MM is included in the overall GABA+ signal. This fraction depends both on the specifics of the editing pulses and the choice of fitting parameters in LCModel, such as the analysis range (MRSI vs. SVS = 1.4–4.2 vs. 0.2–4.0 ppm).

Another source of variation comes from the thalamus being close to the edge of the MRSI VOI. For shimming reasons, the boundary of the VOI could not be moved farther in the inferior direction. Therefore, some of the voxels contributing to both the ROI- and ATL-based analyses were on the boundary. Although quality control was performed in the study, it came at the cost of including less thalamic and ROI volume, especially for a lower concentration species like GABA. This could be one contributor to the significant difference between the ATL-based approach and SVS, as well as the ROI-based approach and SVS, for GABA+/tCr values.

Although individual neurochemical signals are subject to T1 relaxation, the difference in TR values chosen for the two sequences (TR = 1600 ms in MRSI; TR = 2000 ms in SVS) should not have much effect on reported neurochemical ratios with respect to tCr. Using literature values for in vivo T1 relaxation times at 3 T (GABA = 1310 ms,[56] thalamic NAA = 1570 ms[57] and tCr = 1450 ms),[58] the differences in GABA+/tCr and tNAA/tCr caused by the TR change are only 0.9% and 0.6%, respectively; these, therefore, can be neglected. Because of the low concentration of NAAG compared with NAA, the effect from the T1 of NAAG is also neglected here.

4.4 | Comparison of the ATL-based approach with other MRSI analysis approaches

Comparing the three different analysis approaches for the MEGA-LASER 3D MRSI data, tNAA/tCr results from the 4VX and ROI approaches were comparable, as the CRLB-based quality control step has less effect on the measurement of these more abundant neurochemicals. However, these tNAA/tCr values are higher than those obtained with the ATL-based method. As noted earlier, the ROI and 4VX volumes both contain some WM, whereas the ATL-based volume is focused on the gray matter (GM) of the thalamus. Because the WM/GM ratio for tNAA/tCr in this area of the brain is ~ 1.2,[59-61] the inclusion of some WM in the measured volume would be expected to yield a somewhat higher overall tNAA/tCr value.

On the other hand, the lower GABA+/tCr value found using the ATL-based approach versus the other techniques, as seen in Table 2A, was not initially expected, because GABA (GM)/GABA (WM) ratios have been reported to be larger than one[62] ranging from 2 to 8.7.[63-68] Moreover, it is believed that the thalamus has similar or higher GABA+/tCr levels than cortical brain regions,[26,66] which have been the primary focus of GABA comparisons in GM versus WM. However, a recent investigation[69] using the same MEGA-LASER 3D MRSI sequence as that employed here found higher GABA+ in WM instead, possibly due to a higher level of MM signal at 3.0 ppm in WM than in GM.[70] This finding is consistent with our ROI (and 4VX) versus ATL-based results for GABA+/tCr.

As can be observed from Table 3, for each neurochemical, the correlations between the three quantification methods for MRSI data are much more significant than the correlations between SVS and MRSI. The difference to SVS persisted despite extensive testing with different LCModel control parameters for SVS fitting (ie, variation of the analysis window, baseline stiffness, metabolite list, and inclusion or exclusion of a correction term for the CH_2 moiety in creatine). On the other hand, the excellent correlation of the different MRSI processing methods suggests that no significant errors were introduced by going from straightforward manual voxel selection to either of the two automated techniques that both involve registration of interpolated metabolite maps (as well as FreeSurfer-based segmentation in the case of the ATL-based approach).

4.5 | The absence of correlation in Glx

Neither Glx nor Glx/tCr values showed any significant relationship between measurements from the two scan techniques. There are two likely reasons for this discrepancy. First, the different specified editing bandwidths (SV vs. MRSI = 0.36 vs. 0.49 ppm) yield a different range of editing efficiencies, even although Gaussian pulses were used in both sequences, with the editing frequencies, TE value and localization offset frequency optimized for GABA, not Glx. Second, the chemical shift displacement associated with MEGA-PRESS gives rise to a four-compartment effect,[12] in

which coupled "passive" spins in different locations within the voxel experience the effect of refocusing pulses differently. (By contrast, chemical shift displacements are negligible for MEGA-LASER.) The extent of the displacement is greater for the difference spectrum peaks of both Glu (C2 vs. C3 shift difference = 3.74-~ 2.08 ppm = 1.66 ppm) and Gln (1.63 ppm) than for the edited GABA peak (C4 vs. C3 shift difference = 3.01–1.89 ppm = 1.12 ppm). However, the four-compartment effect was not incorporated in the LCModel MEGA-PRESS basis set we used. The lack of correlation between MEGA-PRESS SV and MEGA-LASER MRSI results for Glx and Glx/tCr is likely due to the combination of these editing and processing discrepancies.

4.6 | Limitations

One limitation of this study is that the point spread function (PSF) for MRSI has not been taken into account. However, the effect of the PSF is reduced when neurochemical ratios are considered. In addition, the PSF of the spiral encoding technique used in this MRSI sequence was reported to be close to 1.[25,58] Therefore, the PSF is not expected to cause much variation in the results.

Another limitation is that a water reference scan for the MEGA LASER 3D MRSI sequence was not acquired in this study. Therefore, water scaling for the neurochemical levels measured with MRSI could not be applied. However, the highly significant linear correlation of both raw neurochemical values and ratios to tCr as measured by the two localization techniques has provided a strong cross-validation between the two approaches.

5 | CONCLUSION

This study cross-validated MEGA-LASER 3D MRSI with the commonly used SV MEGA-PRESS sequence for GABA+ measurement by demonstrating a significant correlation of neurochemical levels measured with the two techniques. A new ATL-based MRSI analysis approach was demonstrated, which provides average neurochemical levels for specific brain ROIs by using segmented masks of the structures of interest in native space. This structure-specific approach yielded better reproducibility on test–retest data than by manually choosing MRSI voxels, and even works for MRSI data with only cm-level resolution. The new analysis approach should facilitate the use of the 3D MEGA-LASER MRSI technique in studies comparing GABA levels across populations with better accuracy than using typical ROI analysis methods. However, MRSI voxels crossing the edges of the excitation VOI should be carefully treated when included for quantification purposes, and results should be carefully interpreted by taking the signal decrease as a function of the excitation profile into account. The validation of the 3D MEGA-LASER MRSI results, especially using the new ATL-based approach, versus those from the widely used SV MEGA-PRESS technique, will enable users to understand how changing to a 3D MRSI technique may influence compatibility with prior studies performed with SV MRS.

ACKNOWLEDGEMENTS

The authors give special thanks to Sandy Snyder for the recruitment of the subjects and Dr. Bernhard Strasser for the help with the postprocessing of the MRSI data.

The study was supported by NIEHS #R01 ES020529.

ORCID

Ruoyun E. Ma https://orcid.org/0000-0002-1264-2858
Wolfgang Bogner https://orcid.org/0000-0002-0130-3463
Ulrike Dydak https://orcid.org/0000-0003-1852-7110

REFERENCES

1. Schür RR, Draisma LWR, Wijnen JP, et al. Brain GABA levels across psychiatric disorders: A systematic literature review and meta-analysis of 1H-MRS studies. *Hum Brain Mapp*. 2016;37(9):3337-3352.
2. Duncan NW, Wiebking C, Northoff G. Associations of regional GABA and glutamate with intrinsic and extrinsic neural activity in humans-A review of multimodal imaging studies. *Neurosci Biobehav Rev*. 2014;47:36-52.
3. Sumner P, Edden RAE, Bompas A, Evans CJ, Singh KD. More GABA, less distraction: A neurochemical predictor of motor decision speed. *Nat Neurosci*. 2010;13(7):825-827.
4. Kim S, Stephenson MC, Morris PG, Jackson SR. TDCS-induced alterations in GABA concentration within primary motor cortex predict motor learning and motor memory: A 7 T magnetic resonance spectroscopy study. *Neuroimage*. 2014;99:237-243.
5. Floyer-Lea A, Wylezinska M, Kincses T, Matthews PM. Rapid modulation of GABA concentration in human sensorimotor cortex during motor learning. *J Neurophysiol*. 2006;95(3):1639-1644.
6. Stagg CJ, Bachtiar V, Johansen-Berg H. The role of GABA in human motor learning. *Curr Biol*. 2011;21(6):480-484.

7. Emir UE, Tuite PJ, Öz G. Elevated pontine and putamenal GABA levels in mild–moderate Parkinson disease detected by 7 Tesla proton MRS. *PLoS ONE*. 2012;7(1):e30918.
8. Bai X, Edden RAE, Gao F, et al. Decreased γ-aminobutyric acid levels in the parietal region of patients with Alzheimer's disease. *J Magn Reson Imaging*. 2015;41(5):1326-1331.
9. Chen CMA, Stanford AD, Mao X, et al. GABA level, gamma oscillation, and working memory performance in schizophrenia. *NeuroImage Clin*. 2014;4:531-539.
10. Mescher M, Merkle H, Kirsch J, Garwood M, Gruetter R. Simultaneous in vivo spectral editing and water suppression. *NMR Biomed*. 1998;11(6):266-272.
11. Edden RAE, Barker PB. Spatial effects in the detection of γ-aminobutyric acid: Improved sensitivity at high fields using inner volume saturation. *Magn Reson Med*. 2007;58(6):1276-1282.
12. Marsman A, Mandl RCW, Klomp DWJ, et al. GABA and glutamate in schizophrenia: A 7 T 1H-MRS study. *NeuroImage Clin*. 2014;6:398-407.
13. Mullins PG, McGonigle DJ, O'Gorman RL, et al. Current practice in the use of MEGA-PRESS spectroscopy for the detection of GABA. *Neuroimage*. 2014;86:43-52.
14. Foerster BR, Carlos RC, Dwamena BA, et al. Multimodal MRI as a diagnostic biomarker for amyotrophic lateral sclerosis. *Ann Clin Transl Neurol*. 2014;1(2):107-114.
15. Harris AD, Puts NAJ, Anderson BA, et al. Multi-regional investigation of the relationship between functional MRI blood oxygenation level dependent (BOLD) activation and GABA concentration. *PLoS ONE*. 2015;10(2):1-17.
16. Andronesi OC, Ramadan S, Ratai EM, Jennings D, Mountford CE, Sorensen AG. Spectroscopic imaging with improved gradient modulated constant adiabaticity pulses on high-field clinical scanners. *J Magn Reson*. 2010;203(2):283-293.
17. Hess AT, Dylan Tisdall M, Andronesi OC, Meintjes EM, Van Der Kouwe AJW. Real-time motion and B0 corrected single voxel spectroscopy using volumetric navigators. *Magn Reson Med*. 2011;66(2):314-323.
18. Ebel A, Maudsley AA. Detection and correction of frequency instabilities for volumetric 1H echo-planar spectroscopic imaging. *Magn Reson Med*. 2005;53(2):465-469.
19. El-Sharkawy AEM, Schär M, Bottomley PA, Atalar E. Monitoring and correcting spatio-temporal variations of the MR scanner's static magnetic field. *Magn Reson Mater Physics, Biol Med*. 2006;19(5):223-236.
20. Bogner W, Gagoski B, Hess AT, et al. 3D GABA imaging with real-time motion correction, shim update and reacquisition of adiabatic spiral MRSI. *Neuroimage*. 2014;103:290-302.
21. Garwood M, DelaBarre L. The return of the frequency sweep: Designing adiabatic pulses for contemporary NMR. *J Magn Reson*. 2001;153(2):155-177.
22. Zhu H, Barker PB. MR Spectroscopy and Spectroscopic Imaging of the Brain. In: Modo M, Bulte JWM, eds. *Magnetic Resonance Neuroimaging: Methods and Protocols*. Totowa, NJ: Humana Press; 2011:203-226.
23. Andronesi OC, Gagoski BA, Sorensen AG. Neurologic 3D MR spectroscopic imaging with low-power adiabatic pulses and fast spiral acquisition. *Radiology*. 2012;262(2):647-661.
24. Hnilicová P, Považan M, Strasser B, et al. Spatial variability and reproducibility of GABA-edited MEGA-LASER 3D-MRSI in the brain at 3 T. *NMR Biomed*. 2016;29(11):1656-1665.
25. Henry P, Dautry C, Hantraye P, Bloch G. Brain GABA editing without marcromolecule contamination. *Magn Reson Med*. 2001;45(3):517-520.
26. Behar KL, Rothman DL, Spencer DD, Petroff OAC. Analysis of macromolecule resonances in 1H NMR spectra of human brain. *Magn Reson Med*. 1994;32(3):294-302.
27. McLean MA, Simister RJ, Barker GJ, Duncan JS. Discrimination between neurochemical and macromolecular signals in human frontal lobes using short echo time proton magnetic resonance spectroscopy. *Faraday Discuss*. 2004;126(1):93-102.
28. Pagan FL, Butman JA, Dambrosia JM, Hallett M. Evaluation of essential tremor with multi-voxel magnetic resonance spectroscopy. *Neurology*. 2003;60(8):1344-1347.
29. Weber-Fahr W, Ende G, Braus DF, et al. A fully automated method for tissue segmentation and CSF-correction of proton MRSI metabolites corroborates abnormal hippocampal NAA in schizophrenia. *Neuroimage*. 2002;16(1):49-60.
30. Biedermann SV, Weber-Fahr W, Demirakca T, et al. 31 P RINEPT MRSI and VBM reveal alterations in brain aging associated with major depression. *Magn Reson Med*. 2015;73(4):1390-1400.
31. Ding XQ, Maudsley AA, Sabati M, Sheriff S, Dellani PR, Lanfermann H. Reproducibility and reliability of short-TE whole-brain MR spectroscopic imaging of human brain at 3 T. *Magn Reson Med*. 2015;73(3):921-928.
32. Goryawala MZ, Sheriff S, Maudsley AA. Regional distributions of brain glutamate and glutamine in normal subjects. *NMR Biomed*. 2016;29(8):1108-1116.
33. Schreiner SJ, Kirchner T, Wyss M, et al. Low episodic memory performance in cognitively normal elderly subjects is associated with increased posterior cingulate gray matter N-acetylaspartate: a 1 H MRSI study at 7 Tesla. *Neurobiol Aging*. 2016;48:195-203.
34. Donadieu M, Le Fur Y, Lecocq A, et al. Metabolic voxel-based analysis of the complete human brain using fast 3D-MRSI: Proof of concept in multiple sclerosis. *J Magn Reson Imaging*. 2016;44(2):411-419.
35. Ma R, Bogner W, Andronesi OC, Dydak U. Brain-structure-specific metabolite quantification of MEGA-LASER 3D MRSI data. *Proc Intl Soc Mag Reson Med 25*. 2017:1254.
36. Ma RE, Ward EJ, Yeh CL, et al. Thalamic GABA levels and occupational manganese neurotoxicity: Association with exposure levels and brain MRI. *Neurotoxicology*. 2018;64:30-42.
37. Long Z, Li XR, Xu J, et al. Thalamic GABA predicts fine motor performance in manganese-exposed smelter workers. *PLoS ONE*. 2014;9(2):1-7.
38. Dydak U, Jiang YM, Long LL, et al. In vivo measurement of brain GABA concentrations by magnetic resonance spectroscopy in smelters occupationally exposed to manganese. *Environ Health Perspect*. 2011;119(2):219-224.
39. Arcelli P, Frassoni C, Regondi MC, De Biasi S, Spreafico R. GABAergic neurons in mammalian thalamus: A marker of thalamic complexity? *Brain Res Bull*. 1997;42(1):27-37.
40. Antal M, Beneduce BM, Regehr WG. The substantia nigra conveys target-dependent excitatory and inhibitory outputs from the basal ganglia to the thalamus. *J Neurosci*. 2014;34(23):8032-8042.

41. Graybiel AM. The Basal Ganglia. *Curr Biol*. 2000;10(14):R509-R511.
42. Heckova E, Považan M, Strasser B, et al. Real-time correction of motion and imager instability artifacts. *Radiology*. 2018;286:666-675.
43. Mikkelsen M, Barker PB, Bhattacharyya PK, et al. Big GABA: Edited MR spectroscopy at 24 research sites. *Neuroimage*. 2017;159:32-45.
44. Lange T, Ko CW, Lai PH, Dacko M, Tsai SY, Buechert M. Simultaneous detection of valine and lactate using MEGA-PRESS editing in pyogenic brain abscess. *NMR Biomed*. 2016;29(12):1739-1747.
45. Long Z, Dyke JP, Ma R, Huang CC, Louis ED, Dydak U. Reproducibility and effect of tissue composition on cerebellar γ-aminobutyric acid (GABA) MRS in an elderly population. *NMR Biomed*. 2015;28(10):1315-1323.
46. Provencher SW. Estimation of metabolite concentrations from localized in vivo proton NMR spectra. *Magn Reson Med*. 1993;30(6):672-679.
47. Murdoch JB. Computer studies of multiple-quantum spin dynamics. Lawrence Berkeley Laboratory, University of California. The report number is LBL-15254 1982. https://doi.org/10.2172/6181465
48. Govindaraju V, Young K, Maudsley AA. Proton NMR chemical shifts and coupling constants for brain metabolites. *NMR Biomed*. 2000;13:129-153.
49. Near J, Evans CJ, Puts NAJ, Barker PB, Edden RAE. J-difference editing of gamma-aminobutyric acid (GABA): Simulated and experimental multiplet patterns. *Magn Reson Med*. 2013;70(5):1183-1191.
50. Fischl B, Salat DH, Busa E, et al. Whole brain segmentation: Automated labeling of neuroanatomical structures in the human brain. *Neuron*. 2002;33 (3):341-355.
51. Fischl B, Salat DH, Van Der Kouwe AJW, et al. Sequence-independent segmentation of magnetic resonance images. *Neuroimage*. 2004;23:S69-S84.
52. Razali NM, Wah YB. Power comparisons of Shapiro–Wilk, Kolmogorov–Smirnov, Lilliefors and Anderson-Darling tests. *J Stat Model Anal*. 2011;2(1): 21-33.
53. Di Pietro F, Macey PM, Rae CD, et al. The relationship between thalamic GABA content and resting cortical rhythm in neuropathic pain. *Hum Brain Mapp*. 2018;39(5):1945-1956.
54. Casjens S, Dydak U, Dharmadhikari S, et al. Association of exposure to manganese and iron with striatal and thalamic GABA and other neurometabolites — Neuroimaging results from the WELDOX II study. *Neurotoxicology*. 2018;64:60-67.
55. Yildiz A, Quetscher C, Dharmadhikari S, et al. Feeling safe in the plane: Neural mechanisms underlying superior action control in airplane pilot trainees-A combined EEG/MRS study. *Hum Brain Mapp*. 2014;35(10):5040-5051.
56. Puts NAJ, Barker PB, Edden RAE. Measuring the longitudinal relaxation time of GABA in vivo at 3 Tesla. *J Magn Reson Imaging*. 2013;37(4):999-1003.
57. Ethofer T, Mader I, Seeger U, et al. Comparison of longitudinal metabolite relaxation times in different regions of the human brain at 1.5 and 3 Tesla. *Magn Reson Med*. 2003;50(6):1296-1301.
58. Valkovič L, Chmelík M, Meyerspeer M, et al. Dynamic 31P–MRSI using spiral spectroscopic imaging can map mitochondrial capacity in muscles of the human calf during plantar flexion exercise at 7 T. *NMR Biomed*. 2016;29(12):1825-1834.
59. Gasparovic C, Yeo R, Mannell M, et al. Neurometabolite concentrations in gray and white matter in mild traumatic brain injury: An 1H-magnetic resonance spectroscopy study. *J Neurotrauma*. 2009;26(10):1635-1643.
60. Baker EH, Basso G, Barker PB, Smith MA, Bonekamp D, Horská A. Regional apparent metabolite concentrations in young adult brain measured by 1H MR spectroscopy at 3 Tesla. *J Magn Reson Imaging*. 2008;27(3):489-499.
61. Maudsley AA, Domenig C, Govind V, et al. Mapping of brain metabolite distributions by volumetric proton MR spectroscopic imaging (MRSI). *Magn Reson Med*. 2009;61(3):548-559.
62. Zhu H, Edden RAE, Ouwerkerk R, Barker PB. High resolution spectroscopic imaging of GABA at 3 Tesla. *Magn Reson Med*. 2011;65(3):603-609.
63. Choi IY, Lee SP, Merkle H, Shen J. In vivo detection of gray and white matter differences in GABA concentration in the human brain. *Neuroimage*. 2006;33(1):85-93.
64. Bhattacharyya PK, Phillips MD, Stone LA, Lowe MJ. In vivo magnetic resonance spectroscopy measurement of gray-matter and white-matter gamma-aminobutyric acid concentration in sensorimotor cortex using a motion-controlled MEGA point-resolved spectroscopy sequence. *Magn Reson Imaging*. 2011;29(3):374-379.
65. Jensen JE, Frederick BB, Renshaw PF. Grey and white matter GABA level differences in the human brain using two-dimensional, J-resolved spectroscopic imaging. *NMR Biomed*. 2005;18(8):570-576.
66. Tedeschi G, Bertolino A, Righini A, et al. Brain regional distribution pattern of metabolite signal intensities in young adults by proton magnetic resonance spectroscopic imaging. *Neurology*. 1995;45(7):1384-1391.
67. Choi C, Bhardwaj PP, Kalra S, et al. Measurement of GABA and contaminants in gray and white matter in human brain in vivo. *Magn Reson Med*. 2007; 58(1):27-33.
68. Harris AD, Puts NAJ, Edden RAE. Tissue correction for GABA-edited MRS: Considerations of voxel composition, tissue segmentation, and tissue relaxations. *J Magn Reson Imaging*. 2015;42(5):1431-1440.
69. Považan M, Hnilicová P, Hangel GJ, et al. Detection of MM using metabolite-nulled MEGA-LASER at 3 T – A possible effect on GABA+ signal. *Proc Intl Soc Mag Reson Med 25*. 2017:1058.
70. Moser P, Hingerl L, Strasser B, et al. Whole-slice mapping of GABA and GABA + at 7 T via adiabatic MEGA-editing, real-time instability correction, and concentric circle readout. *Neuroimage*. 2019;184:475-489.

SUPPORTING INFORMATION

Additional supporting information may be found online in the Supporting Information section at the end of this article.

How to cite this article: Ma RE, Murdoch JB, Bogner W, Andronesi O, Dydak U. Atlas-based GABA mapping with 3D MEGA-MRSI: Cross-correlation to single-voxel MRS. *NMR in Biomedicine*. 2021;34:e4275. https://doi.org/10.1002/nbm.4275